ACS Sustainable Chemistry & Engineering

pubs.acs.org/journal/ascecg

Research Article

Predicting Catalytic Pyrolysis Aromatic Selectivity from Pyrolysis Vapor Composition Using Mass Spectra Coupled with Statistical Analysis

Anne K. Starace,* David D. Lee, Kristen T. Hietala, Yeonjoon Kim, Seonah Kim, Anne E. Harman-Ware, and Daniel L. Carpenter

Cite This: https://doi.org/10.1021/acssuschemeng.1c05916

Read Online

ACCESS | Metrics & More | Article Recommendations | Supporting Information

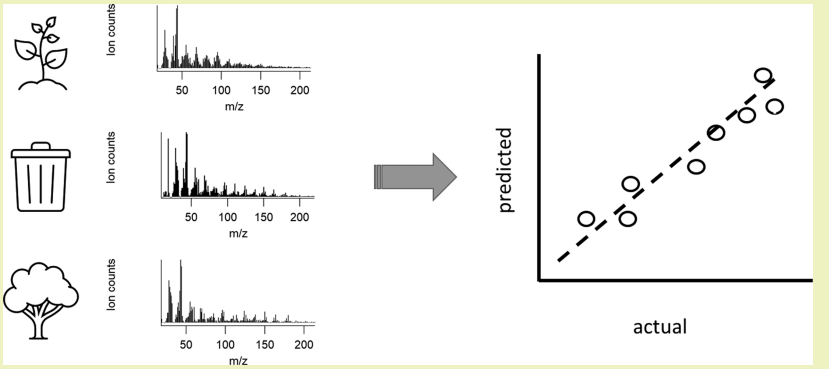

ABSTRACT: The behavior of fast pyrolysis (FP) and catalytic FP (CFP) of 20 renewable feedstocks was studied in a microscale reactor with molecular beam mass spectral analysis of products generated. A partial least-squares (PLS) model was constructed based on the FP vapor spectra that predicts the aromatic selectivity when upgrading over a ZSM-5 catalyst. Additionally, principal component analysis of both FP and CFP spectra was performed for comprehensive spectral analysis. This work highlighted the value of vapor-phase mass spectral screening to predict the subsequent feedstock performance and demonstrated that the quantity of coke deposited on the catalyst is not a reliable measure of catalyst deactivation when the feedstock type is varied.

KEYWORDS: *catalytic fast pyrolysis, HZSM-5, partial least squares, biomass feedstocks, principal component analysis, bio-oil*

INTRODUCTION

The production of fuels and chemicals from renewable, non-fossil-based sources is necessary both to eliminate dependence on crude oil and to mitigate climate change. Catalytic fast pyrolysis (CFP) is one technology that can potentially use a variety of bioderived feedstocks (forest thinnings, agricultural waste, municipal solid waste, etc.) to accomplish this goal. The predominant focus of CFP research has been on the development of catalysts and process conditions, and relatively less work has been focused on the effect of variable feedstocks on the CFP product yields and distributions. Furthermore, much of the work probing CFP reaction mechanisms has been performed, understandably, on model compounds. It is largely unknown how interactions, if present, between the hundreds of compounds generated from raw, uncatalyzed pyrolysis of biomass affect the CFP products. One approach to determine how pyrolysis vapor composition from real biomass affects the catalytic pyrolysis products is to study a large variety of feedstocks and use chemometrics and machine learning techniques to analyze the data.

A handful of studies wherein multiple feedstocks are upgraded over the ZSM-5 catalyst using the same process conditions have been performed. Mihalcik et al. have studied eight feedstocks (corn cob, corn stover, switchgrass, oak, cellulose, xylan, pure lignin, and ETEK lignin) over HZSM-5 at a 1:5 biomass-to-catalyst ratio at 550 °C.[1] Of the whole feedstocks, switchgrass produces about two-thirds the amount of benzene of the rest of the feedstocks but around 1.5 times the toluene and over 5 times the amount of ethyl benzene. Oak produced the most p-xylene (4.12 wt %), followed by corn cob and corn stover (3.49−3.65 wt %) with switchgrass producing the least (2.56 wt %). Switchgrass produced about two-thirds the amount of naphthalene and methyl naphthalene as the

Received: August 29, 2021
Revised: December 10, 2021

other feedstocks. Mante and Agblevor performed pilot-scale CFP with ZSM-5 at 550 °C with a biomass-to-catalyst ratio of 0.1 using six different feedstocks (hybrid poplar, pine, pinyon−juniper mixture, switchgrass, corn stover, and pine bark).[2] The pine bark produced the most coke and char (33.4 wt %), while hybrid poplar produced the least (17 wt %). The overall H/C molar ratios of the oils produced ranged from 0.98 to 1.1, with corn stover and switchgrass having the lowest and highest values, respectively. The pH of the liquid products ranged from 3.71 (pine) to 4.99 (switchgrass). Complementary microscale experiments investigating detailed chemical composition were also performed, and the distribution of aromatic products was more similar between corn stover and switchgrass compared with the work of Mihalcik et al. where more significant differences were found. Wang et al. performed small-scale CFP experiments at 500 °C using "a spray-dried, non-zeolitic, alumina-based catalyst" with seven different feedstocks.

The yields of organic liquids ranged from 14 to 20.8 weight percent, and *Arundo donax* and miscanthus stood out as having the highest values, both above 20 wt %.[3] The organic content of the organic liquid phase ranged from 75 to 82.7 weight percent, with *A. donax* having this highest value and corn stover the lowest. The total aromatic yield ranged from 26.2 to 38.9 peak area percent, and the values were evenly spaced over this range.

From these studies, we see that the yields, the chemical composition of products, and the bulk oil properties from CFP are feedstock dependent. Wang et al. noticed a strong negative correlation between the hemicellulose content of the feedstock and the amount of CO produced during CFP.[3] Mante and Agblevor found that methoxylated phenolics in biomass are generally aromatized less than non-methoxylated phenolics over ZSM-5.[2] However, an additional experimental work is needed to better understand the effect of feedstock composition and subsequent raw pyrolysis intermediates on CFP upgrading products so that CFP products can be estimated in advance based on feedstock properties, and high-throughput methods are best suited for this. Furthermore, rapid screening of feedstocks to predict their upgrading performance would be beneficial to biorefineries as it would enable them to take into account the performance of the feedstock in addition to cost and availability in their calculations. This is critical as the cost of the feedstock itself is currently estimated to be the largest single cost of a biorefinery, as a model of de-barked pine CFP indicates.[4]

Rapid screening of feedstock pyrolysis vapors with molecular beam mass spectrometry (MBMS) has proven to be a valuable tool to measure the feedstock chemical properties once sufficient data has been collected to calibrate the methods. For example, the determination of the S, G, and H lignin content via wet chemical methods requires days,[5,6] whereas methods to determine the lignin content and monomer ratios via MBMS analysis of pyrolysis vapors has successfully reduced analysis time to minutes.[7,8] If analysis of biomass pyrolysis vapors can be used to determine the chemical composition of the biomass prior to deconstruction, it is expected that this technique can also be used to predict CFP products once sufficient data is collected using the relevant catalyst(s) and upgrading conditions.

To enable this, a comprehensive analysis of large MBMS spectral data sets can be achieved using factor analysis, discriminant analysis, and principal component analysis (PCA) to elucidate underlying data structures and variations in the feedstock and analyte composition.[9−11] Nonetheless, the high dimensionality of MBMS data (i.e., the large number of peak intensities for each sample and the potentially multiple biopolymer sources for each ion) remains a challenge, especially in experimental sets with fewer unique spectra. Jarvis et al. carried out the FP of oak at different temperatures (450−950 °C) and obtained six principal component mass spectra, representing the major products at different temperatures.[12] Mukarakate et al. analyzed the mass spectra from upgrading pine pyrolysis vapors over HZSM-5 using PCA to investigate different product compositions as the catalyst deactivated.[13] Recently, PCA has been successfully applied to elucidate genotype effects on lignin composition[9] and the machine learning-based classification of pyrolysis MBMS data of lignocellulosic biomass.[14] All these studies indicate that the PCA method can be applied when scrutinizing the feedstock effect on the product selectivity of CFP.

Partial least-squares regression (PLS) models have been built using pyrolysis MBMS data to predict biomass composition with differing degrees of success.[15,16] The use of PLS models to link FP MBMS data relating to the composition of feedstocks and their raw vapor products with their respective upgraded products could provide new insights and opportunities for understanding feedstock impacts on thermocatalytic conversion paradigms.

In this work, we pyrolyzed 20 feedstocks and upgraded the vapors over the ZSM-5 catalyst in eight pulses for a cumulative biomass-to-catalyst ratio of one while collecting the mass spectra of the vapor-phase products in real time prior to condensation. Pyrolysis vapor-phase mass spectra were also collected for each feedstock with no catalytic upgrading. A PLS model was used to predict the aromatic selectivity, as measured by the upgraded spectra, from the raw pyrolysis vapor spectra. Data were also analyzed using PCA.

MATERIALS AND METHODS

Materials. Feedstocks were provided by Idaho National Laboratory, with the exception of Avicel, which was purchased from Sigma-Aldrich and pine lignin, which was isolated at NREL. The milled wood lignin was prepared from extractive-free loblolly pine according to the Bjorkman method.[17,18] More details on the lignin isolation process are provided in the Supporting Information.

All feedstocks were knife-milled to a 2 mm screen size. The feedstocks are shown in Table 1 along with their abbreviations used here. Feedstocks were chosen to make up a varied set of starting compositions for model development; the cost and availability of the feedstocks are not considered in this work. The ZSM-5 catalyst was purchased from Zeolyst (CBV 3024E) and had a silica-to-alumina ratio of 30.

METHODS

Experimental Section. NREL's py-MBMS system has been described in detail previously.[19] However, in this work, we used a modified quartz reactor which allows for more facile insertion and removal of the catalyst. A schematic diagram of this reactor is shown in Figure 1a along with the pictures of the catalyst shuttle (b) and the insertion of biomass into the reactor (c and d).

Using the reactor shown in Figure 1, catalytic FP was performed *ex situ* in sequential batch pulses with both the pyrolysis and catalyst bed temperatures at 500 °C. Biomass [30 mg (±0.03 mg)] was pyrolyzed per pulse over a 240 mg packed catalyst bed. The carrier gas was 400 sccm helium, and a diluent gas (4,000 sccm He) was added after the catalyst bed before MBMS sampling.

Each experiment consisted of pyrolyzing a pulse of biomass with no catalyst in place, inserting the catalyst, allowing the catalyst to

https://doi.org/10.1021/acssuschemeng.1c05916
ACS Sustainable Chem. Eng. XXXX, XXX, XXX−XXX

Table 1. Feedstock Abbreviations

feedstock	abbreviation
air-classified forest residue	acFR
Avicel	Avi
clean paper	ClPa
construction and demolition waste	CD
corn stover	CS
eucalyptus	EUC
forest residue	FR
grass clippings	GrCl
hybrid poplar	HP
loblolly pine	LLYP
Miscanthus	MISC
mixed grasses	MG
oriented strand board	OSB
pine lignin	PLig
pinyon/juniper	PJ
reed canary	ReCa
shrub willow	SW
switchgrass	SG
tulip poplar	TP
white oak	WO

thermally equilibrate, pyrolyzing eight pulses of biomass over the catalyst (biomass-to-catalyst ratio (B/C) 0.125 to 1), removing the catalyst bed, and pyrolyzing one final pulse of biomass with no catalyst present.

The coked catalyst samples produced from 10 feedstocks (LLYP, WO, PJ, MG, EUC, OSB, TP, CS, Avi, and PLig) were cooled under a flow of inert gas and subsequently analyzed with a thermal gravimetric analyzer (TGA) to measure the total mass of coke deposited.

Ultimate analysis of the feedstocks was performed with a LECO CHN determinator using high-temperature combustion, followed by infrared analysis. Proximate analysis was performed with a LECO carousels TGA using ASTM ASTM-D7582-12. Proximate and ultimate analysis data are reported here on an as-received basis. Some of the proximate and ultimate data has been previously reported on a dry basis.[20−22] Lignin composition was measured via py-MBMS analysis described previously. Briefly, 4 mg of biomass was pyrolyzed at 500 C, and lignin content was determined relative to a relevant standard of known Klason lignin content based on the mean-normalized intensity of ions m/z 120, 124, 137, 138, 150, 152, 154, 164, 167, 168, 178, 180, 181, 182, 194, 208, and 210.[9]

Regression Model. Partial least-squares (PLS) regressions were performed in The Unscrambler X using the Kernel Algorithm and LOO (leave one out) cross-validation. The aromatic sum was calculated by summing the m/z peaks listed in Table 2 over the first pulse of biomass, resulting in a biomass-to-catalyst ratio (B/C) of 0.125. Data from each FP pulse (one before and one after catalytic upgrading) were averaged. To avoid an overdefined system, 20 chemically important peaks from the FP spectra were chosen, shown in Table 3, as input values. While the compounds in Table 3 are by no means an exhaustive list of the relevant pyrolysis products since it needed to be limited to a maximum of 20 compounds, the authors chose compounds they had found to have particular relevance in previous work, as well as being mindful to include compounds from both the carbohydrate and lignin components of biomass. The uncertainty test in The Unscrambler X, which uses a jackknife,[23] was used to determine which regression coefficients were significant.

Table 2. Peaks from Catalytic Pyrolysis Spectra Used for Aromatic Sum

m/z	i.d.
78	benzene
91,92	toluene
106	xylene or ethylbenzene
128	naphthalene
142	methylnaphthalene
156	dimethylnaphthalene and/or ethylnaphthalene

Principal Component Analysis. PCA was carried out using the scikit-learn package[24] in Python 3.7 to analyze the complex patterns of the FP and CFP spectra through dimensionality reduction. Seven principal components were chosen through singular value decom-

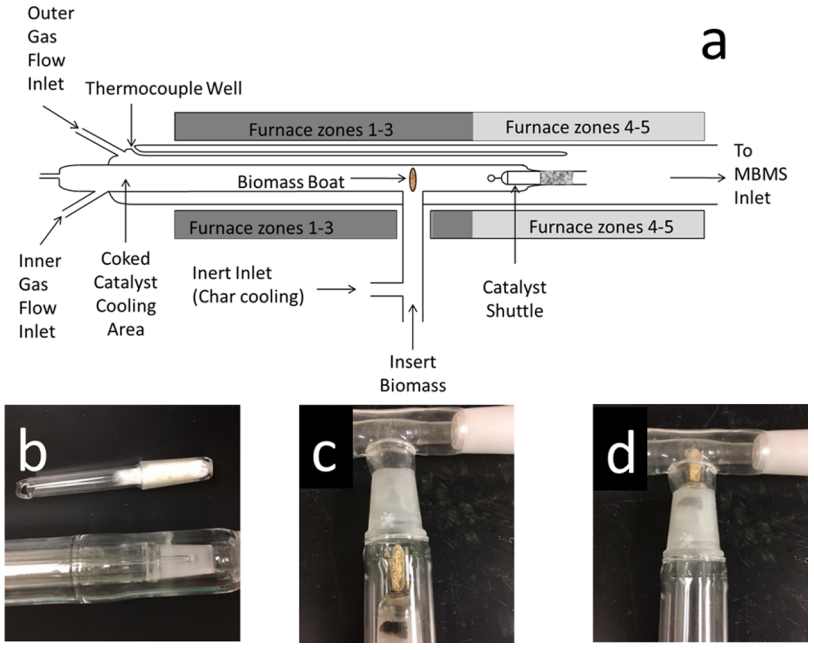

Figure 1. (a) Schematic diagram of the quartz reactor, (b) photograph of the catalyst shuttle alongside a portion of the quartz reactor with a ground glass joint to hold the catalyst shuttle, (c) photograph of the biomass pulse entering the quartz reactor, and (d) photograph of the biomass pulse seated in the quartz reactor. Photographs taken by Anne Starace. Schematic diagram created by David Lee and Anne Starace.

https://doi.org/10.1021/acssuschemeng.1c05916
ACS Sustainable Chem. Eng. XXXX, XXX, XXX−XXX

Table 3. Peaks from Pyrolysis Spectra Used as Predictors in the Model

m/z	i.d.
56	butene
58	acetone, glyoxal, propenol
60	hydroxyacetaldehyde, acetic acid
68	furan
82	methyl furan
94	phenol
96	furfural
98	furfuryl alcohol, 5-methyl-2(3*H*)-furanone
108	cresol
110	catechol
114	methylhydroxyfuranone and/or hydroxydihydropyranone
120	vinylphenol
124	guaiacol
126	hydroxymethyl furfural, maltol
138	methyl guaiacol, hydroxybenzoic acid
144	dianhydro-α-D-glucopyranose
150	vinylguaiacol and/or coumaryl alcohol
154	syringol
164	eugenol and/or coumaric acid
210	sinapyl alcohol

position using the ARPACK solver since at least seven components were required to achieve the sum of the explained variance ratio of 90%. The m/z range of 45−210 was used for the PCA to avoid contributions from noise peaks, water, and air contaminants in the sampling inlet to the mass spectrometer, and the peak intensities of all mass spectra were normalized with respect to the total ion count (TIC) before conducting PCA. The PCA score and loading mass spectra were analyzed for the two principal components (PC 1 and PC 2) that show the highest explained variance. This analysis informs us of the variance of (i) raw FP vapor composition, (ii) product distribution from CFP, and (iii) catalyst deactivation process when different feedstocks are used. More specifically, a small or large distance between data points in the 2D PCA score plot indicates a similar or different vapor composition and catalyst deactivation progress. The key m/z values determining the variance among feedstocks are found through the analysis of loadings calculated by multiplying the square root of the explained variance (eigenvalue) to the principal axis vector (eigenvector).

RESULTS AND DISCUSSION

The experiment flow is shown in Figure 2 using white oak as an example and displaying only a subset of ions tracked. Here, we note that the aromatic sum is small for the FP pulses, much larger in the CFP pulses, and decreases in magnitude as the biomass-to-catalyst ratio increases with subsequent CFP pulses and the catalyst partially deactivates. m/z 60, from hydroxyacetaldehyde and acetic acid, is present in much larger amounts on the FP pulses than the CFP pulses, where both hydroxyacetaldehyde and acetic acid are converted by the catalyst. m/z 82 from methyl furan and cyclopentenone is present in the FP vapors and is present in much lower amounts after passing over the fresh, active catalyst but then is present in larger amounts over the partially deactivated catalyst compared to the vapors with no catalytic upgrading. This could be due to both breakthrough of primary vapors occurring and the production of more methyl furan from the incomplete deoxygenation of furfural as the catalyst is partially deactivated. Similarly, looking at the trace from m/z 94, most likely phenol, we see that phenol is both a primary pyrolysis product and produced by the incomplete deoxygenation of methoxy phenols by a partially deactivated catalyst. In each experiment, the mass spectrum is recorded from 10 to 510 m/z and collected once per second. Spectra were averaged over each pulse and normalized to the TICs.

Figure 3 shows a parity plot of the measured *versus* predicted aromatic sum for a biomass-to-catalyst ratio of 0.125 using the aromatic sum of only the first pulse of biomass vapors over the catalyst. Each point is labeled with the feedstock abbreviation, and the solid line indicates $x = y$. The figure shows some predictive capability from PLS modeling in even a small data set such as this. The regression coefficients that were significantly positively correlated with the aromatic sum were m/z 58 (acetone, glyoxal, and/or propenol), m/z 60 (hydroxyacetaldehyde and/or acetic acid), and m/z 98 (furfuryl alcohol and/or 5-methyl-2(3*H*)-furanone). These

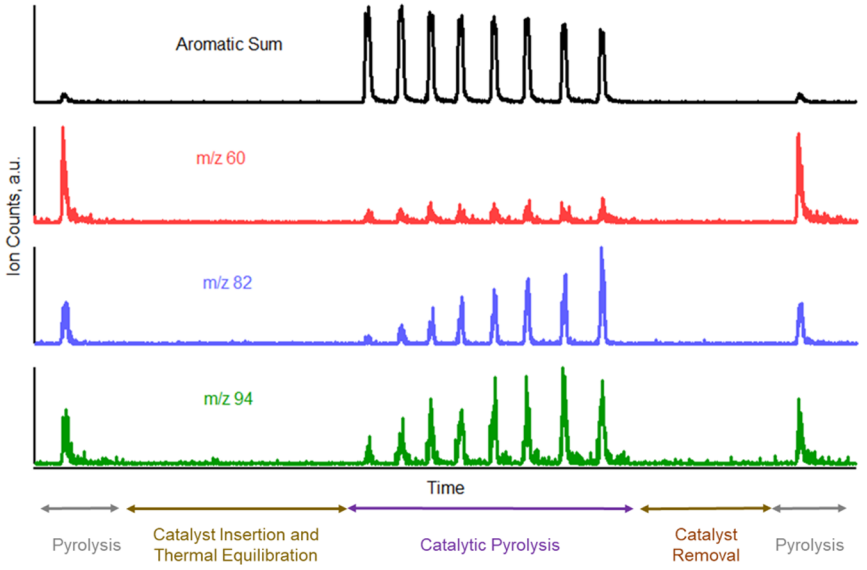

Figure 2. White oak results as an example of experimental data collected with time. Traces of the ion counts of the aromatic sum (top, black trace), m/z 60 (second from top, red trace), m/z 82 (second from bottom, blue trace), and m/z 94 (bottom, green trace).

https://doi.org/10.1021/acssuschemeng.1c05916
ACS Sustainable Chem. Eng. XXXX, XXX, XXX−XXX

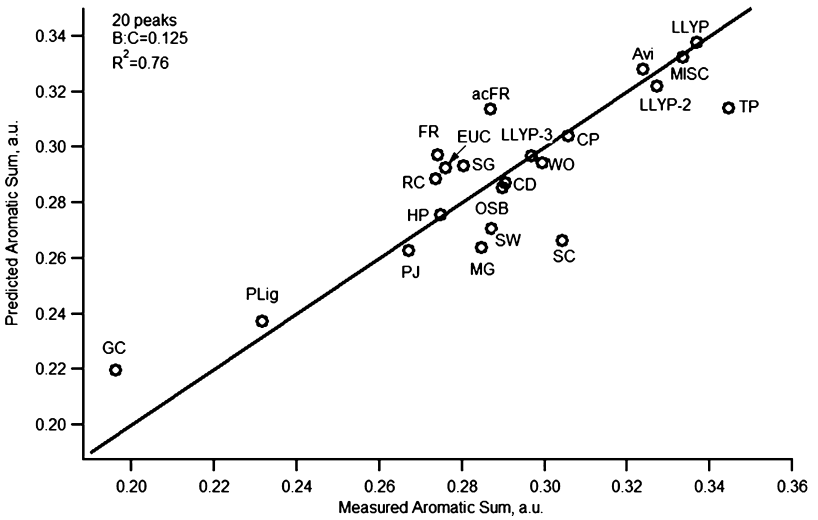

Figure 3. Measured *vs* predicted aromatic sums of each feedstock. The line indicates $x = y$.

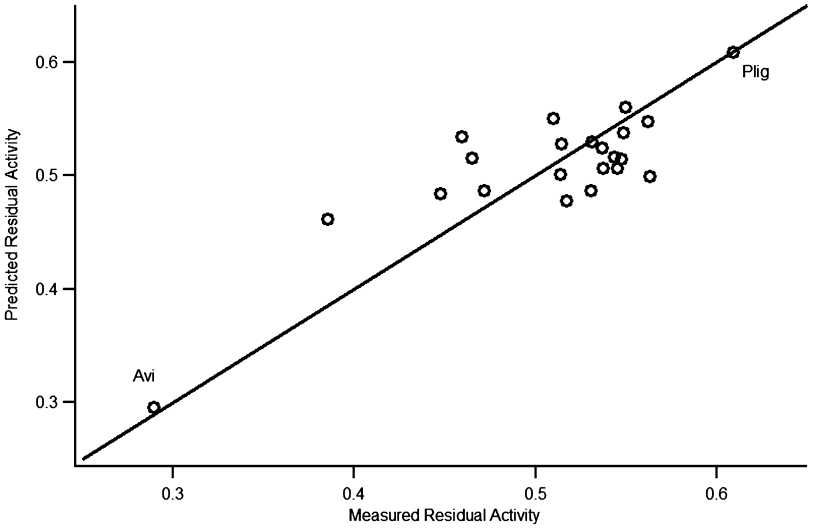

Figure 4. Measured *vs* predicted residual activity. The line indicates $x = y$.

vapors are all primarily produced from the carbohydrate fraction of biomass. The regression coefficients that were negatively correlated with the aromatic sum were m/z 108 (cresol) and m/z 110 (catechol), both primarily sourced from the lignin fraction of biomass. This suggests that over a ZSM-5 catalyst (SAR 30) at 500 °C, the carbohydrate fraction of biomass produces proportionately more aromatics than the lignin fraction and is consistent with previous work analyzing the pyrolysis of biomass fractions upgraded over ZSM-5 in a micropyrolyzer.[25]

To assess the impacts on catalyst deactivation, we chose to measure the catalyst activity by what we have termed the residual activity, which is simply the aromatic sum of the last pulse divided by the aromatic sum of the first pulse.

$$\text{Residual activity} = \frac{\text{aromatic sum last pulse}}{\text{aromatic sum first pulse}}$$

Figure 4 shows the parity plot of the predicted *versus* measured residual activity and shows that this regression is driven almost entirely by the Avicel and pine lignin. We found no statistically significant negative regression coefficients but found that m/z 110 (catechol) and 124 (guaiacol) were significantly positively correlated with the final activity. Both are associated with the lignin fraction of the biomass, suggesting that feedstocks with larger lignin fractions retain aromatic conversion activity to higher B/C than feedstocks with smaller lignin fractions. Additionally, these are small lignin-derived ions (m/z 110 and 124 *vs* m/z 150, 154, 168, 194, and 210), indicating that feedstocks whose lignin components fragment into smaller molecules during pyrolysis result in aromatic activity retained to higher B/C. While we did not find any statistically significant negative regression coefficients, it is generally the case that the carbohydrate and lignin fractions of biomass are inversely proportional; thus, the positive correlation between residual activity and lignin content could be due to proportionately less carbohydrate fraction causing deactivation.

If the primary deactivation mechanism is coking, one would expect the residual activity to be negatively correlated with the mass of coke deposited. This is not the case for the feedstocks where the coke was measured, as shown in Figure SI1 in the Supporting Information. We also found no correlation between the aromatic selectivity, that is, the aromatic sum and the residual activity. This suggests that multiple reaction types lead

https://doi.org/10.1021/acssuschemeng.1c05916
ACS Sustainable Chem. Eng. XXXX, XXX, XXX−XXX

to the deposition of coke, not only reactions that generate aromatic products. Instead, the residual activity was strongly correlated with the amount of vapor produced (as measured by difference from the initial mass of the feedstock and the char and ash remaining) from the pyrolysis of the feedstock, apart from grass clippings, as shown in Figure 5. Grass clippings are

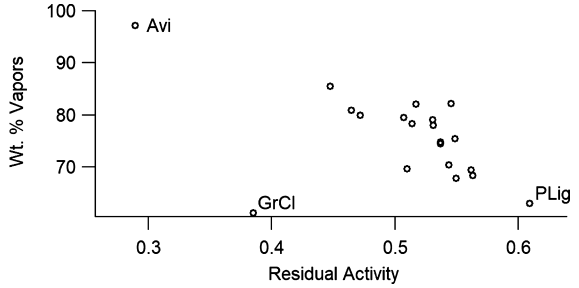

Figure 5. Residual activity of the catalyst plotted against weight percent solids (sum of char and ash) formed during pyrolysis for each feedstock.

the exception to this trend since they create the lowest amount of pyrolysis vapors by weight but also have the second to lowest residual activity, indicating that the grass clipping pyrolysis vapors decrease the activity of the catalyst proportionately more than the other feedstocks studied, which will be discussed in detail, subsequently.

To investigate the unexpected lack of correlation between the final activity of the catalyst and the amount of coke formed on the catalyst, as shown in Figure SI1, we considered the previous work by Stanton et al. They studied the catalytic pyrolysis of southern pine, Avicell, and Organosolv lignin from mixed hardwoods and determined that the carbohydrate fraction of feedstocks formed more coke in the pores of the ZSM-5 catalyst which rapidly decreased its ability to produce aromatics, while the lignin fraction formed coke on the surface of the catalyst which did not significantly hinder the ability of the catalyst to produce aromatics up to a biomass-to-catalyst ratio of 2.[26] If this generalizes to all lignocellulosic biomass, it would suggest that for feedstocks where the ratio of carbohydrates to lignin varies, the coke content would not correlate with the deactivation of ZSM-5 toward aromatic production. Conversely, for feedstocks with similar carbohydrate-to-lignin ratios, a correlation should be observed.

To evaluate why grass clipping pyrolysis vapors cause a relatively faster deactivation, we turn to a PCA of upgraded pyrolysis vapors and raw pyrolysis vapor mass spectra. Figure 6a shows a score plot of the first two principal components of the CFP spectra where the red dots are the average spectra of the first three biomass pulses, the orange dots are the average spectra of the middle two pulses of biomass, and the yellow dots are the average spectra of the final three pulses of biomass. As the catalyst deactivates, the points move from left to right, from a negative value of PC 1 to a positive value. Figure 6b shows the corresponding spectral loadings where PC 1 corresponds to a decrease in upgraded aromatic products (i.e., m/z 82, 91, 106, 128, etc.) and an increase in breakthrough products (including m/z 94, 110, etc.) moving from left to right in the scores plot, accounting for 78% of variance in the spectra. In Figure 6c, it can be seen that the grass clippings stand out in that they display the highest positive values for PC 2 and trend highest in PC 1 in the average of the first three pulses of biomass over the catalyst. PC 2 only explains 8% of the variance in the CFP spectra of which spectral intensities are driven by positive ions m/z 51, 65, 77, 89, 115, 129, and 141 likely corresponding to nitrogenous species (being odd numbered) and/or aromatic aldehydes, ketones, or amides as well as negative ions m/z 68 (furan), 82 (methyl furan) 92, (toluene), and 106 (benzene/xylene). These PC 2 loadings imply a negative correlation between the upgraded products and those potentially originating from nitrogenous or other species. It is noteworthy that the average of the first three pulses of grass clippings shows the same amount of catalyst deactivation (as measured by PC 1) as the final three pulses of biomass from the other feedstocks, despite producing the lowest mass of vapors from each pulse. Furthermore, as more grass clippings are pyrolyzed, and the vapors pass over the catalyst, the catalyst deactivation continues. The grass clipping vapors produce the most catalyst deactivation over the eight pulses.

To understand why the grass clipping pyrolysis vapors cause so much catalyst deactivation, we refer to the spectra of the raw vapors. From a PCA of the FP spectra (shown in Figure 7a), we see that grass clippings have the largest positive value of PC 1 (explaining 26% of the variance) in the scores plot. Looking at the positive loadings for PC 1 in Figure 7b, we see that m/z 59 stands out as a peak that is not typically seen in the pyrolysis of herbaceous or woody biomass.[9] All the possible sources of this peak contain nitrogen, though acetaldoxime is a potential match as it has 59 as its parent peak and has m/z 41 as its largest fragment peak,[27] and 41 is also a large positive peak in the PC 1 loading. This nitrogen-containing peak in the grass clippings' raw pyrolysis spectra is potentially from fertilizers and/or pesticides applied to the grass during growth or otherwise from reactions involving chlorophyll in grass leaves or other contaminants that could originate from the soil. It may be possible that the nitrogen-containing component of the grass clippings could deactivate ZSM-5 more rapidly than the remainder of the components in the pyrolysis vapors. Previous work in the literature has indicated that the nitrogen-containing compounds, particularly nitrogen heterocycles, deactivate zeolite catalysts.[28,29] Additional evidence of the presence of nitrogenous species in the grass clippings can be seen in the actual spectra of the grass clippings (Figure SI2), consisting of large abundances of ions 81 and 95, which, when correlated together, may derive from phytol, generated when chlorophyll pyrolyzes, which provides evidence supporting the presence of chlorophyll in the feedstock. Therefore, the chlorophyll, which produces nitrogenous pyrroles, could potentially lead to deactivation of ZSM-5.[30] Additionally, PC 1 loadings show variance driven by the abundance of (positive) m/z 91, 94, and 120 produced from grass clippings that likely originate from coumarate and/or other phenolic species not necessarily related to lignin.[31] The negative loadings in the PC 1 analyses (implying the negative correlation with the ions 91, 94, and 120) primarily correspond to hemicellulose-derived species such as m/z 114 and lignin-derived species including m/z 124, 138, 164, and 180, indicating that the relative abundance of lignin content in the feedstocks decreases left to right across the score plot. On the other hand, PC 2 is driven (17% variance) by the positive correlation between m/z 95, 96, and 114 (derived from sugars, particularly from the hemicellulose) and 120 against the lignin-derived species (whereas 114 was positively correlated with the lignin species in PC 1 and negatively associated with 95 and 96). This variation is likely related to the biopolymer content, type, and distribution

https://doi.org/10.1021/acssuschemeng.1c05916
ACS Sustainable Chem. Eng. XXXX, XXX, XXX−XXX

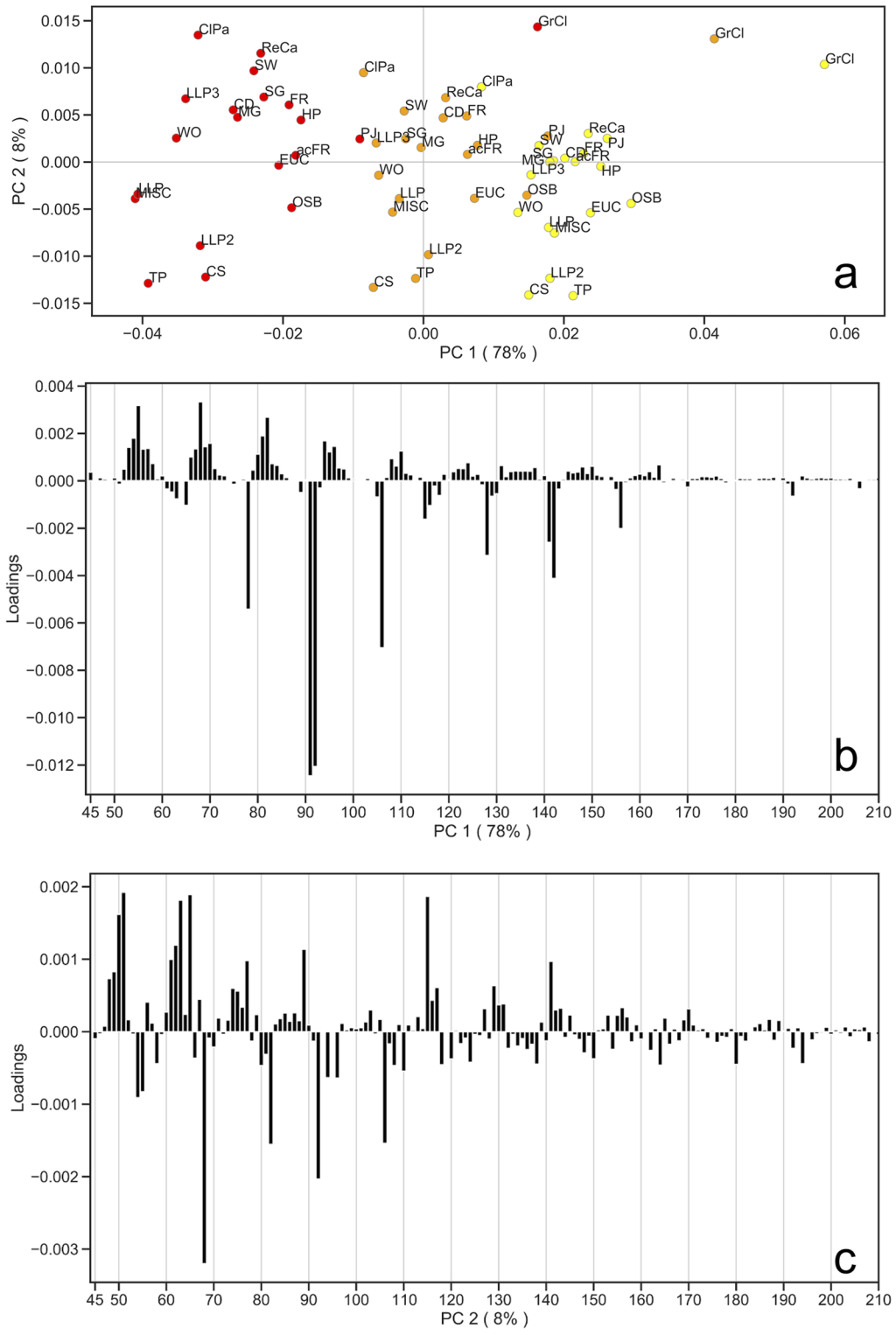

Figure 6. (a) PCA score projection of CFP spectra (m/z 45-210) from the first three pulses of biomass (red dots), the middle two pulses of biomass (orange dots), and the final three pulses of biomass (yellow dots), (b) corresponding PC 1 spectral loadings, and (c) PC 2 spectral loadings for CFP spectra.

in the plant cell walls, which is likely different in structure and composition, particularly for hemicellulose sugars and coumarates and may impact subsequent pyrolysis product distribution. Last, the ultimate analysis of the feedstocks show that grass clippings has by far the largest nitrogen content (3.6% by weight), as can be seen in Table 4.

The large amount of inorganic ash in the grass clippings (12.2 wt % as shown in Table 4) may also provide insight into why the catalyst deactivates more quickly from the grass clipping vapors. As ash species catalyze the thermal degradation of carbohydrates in the biomass,[32,33] there is a higher relative production of carbohydrate-derived species such as 58, 60, and so forth, which we also demonstrated to

https://doi.org/10.1021/acssuschemeng.1c05916
ACS Sustainable Chem. Eng. XXXX, XXX, XXX−XXX

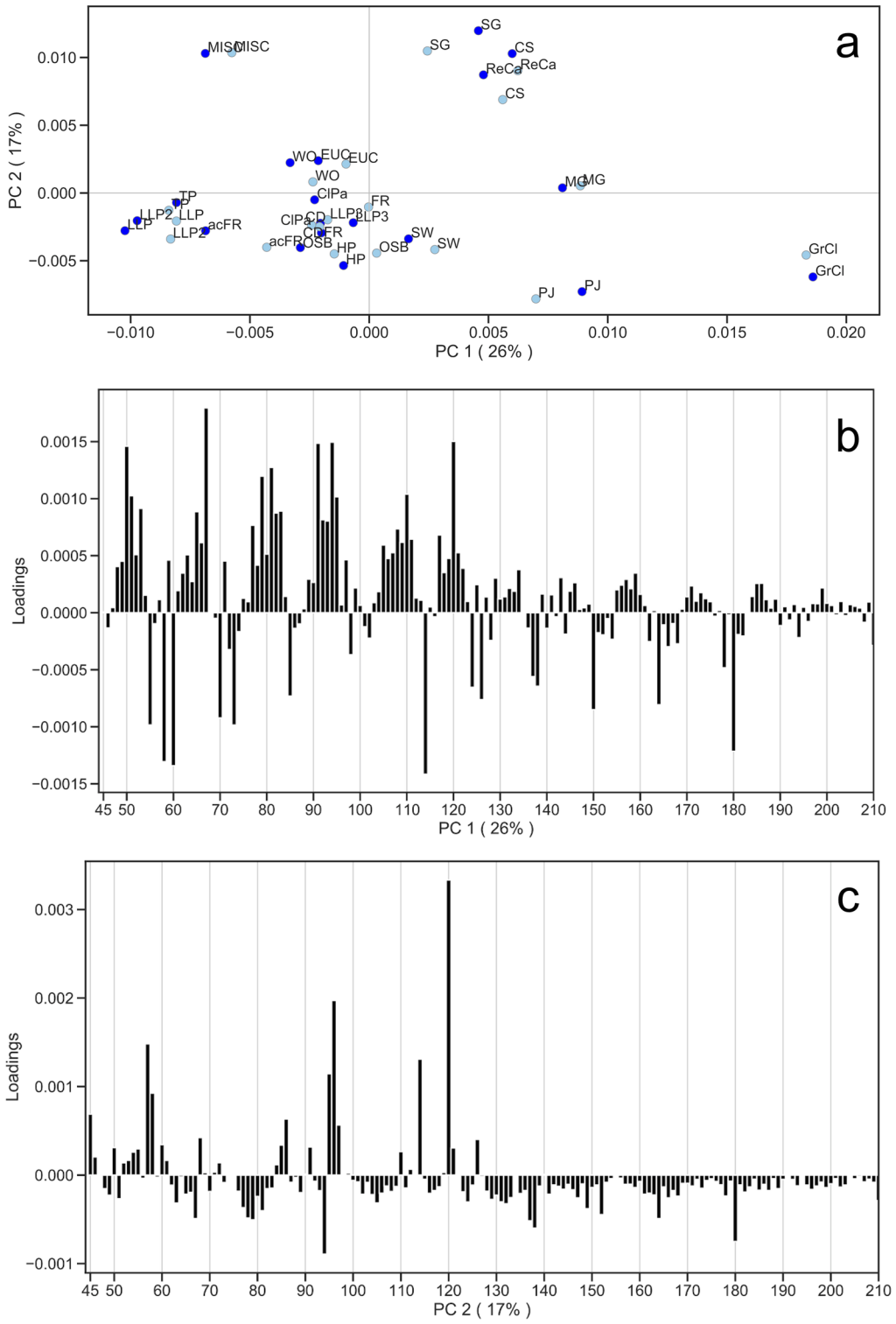

Figure 7. (a) PCA score projection of FP spectra (m/z 45-210) from the biomass feedstocks, (b) corresponding PC 1 spectral loadings, and (c) PC 2 spectral loadings for FP spectra. Replicate analyses are included.

correlate with catalytic conversion and the initial higher production of these components from grasses may lead to shorter catalyst lifetime. Other large positive peaks in PC 1 correspond to coumarate and coumaryl lignin (91, 94, and 120), which is unsurprising as herbaceous feedstocks typically have a much higher proportion of H lignin and coumarates than woody feedstocks[34] and also have lower S/G ratios (higher coniferyl lignin relative to syringyl lignin) than hardwoods (67, 95).[31,35−37]

CONCLUSIONS

The transition to using renewable feedstocks for the scaled production of fuels and chemicals will require the widespread use of potentially heterogeneous feedstocks (municipal solid waste, wet waste, agricultural residues, forest thinnings, etc.).

https://doi.org/10.1021/acssuschemeng.1c05916
ACS Sustainable Chem. Eng. XXXX, XXX, XXX−XXX

Table 4. Weight Percent of Carbon, Hydrogen, Nitrogen, and Ash in Feedstocks on an As-Received Basis[a]

	wt %				
feedstock	C	H	N	Ash	Lignin
acFR	51.4	6.7	0.1	1.2	28.2
Avi	44.4	6.1	0.5	NA	NA
ClPa	39.0	5.3	0.0	13.3	12.7
CD	0.5	0.1	0.0	1.6	21.4
CS	39.8	5.5	0.9	9.7	14.8
EUC	ND	ND	ND	1.4	24.4
FR	47.7	6.4	0.2	4.5	26.7
GrCl	36.5	5.6	3.6	12.2	14.7
HP	48.1	6.0	0.2	1.2	23.5
LLYP	48.7	6.7	0.1	BDL	29.8
MISC	50.6	5.9	0.2	1.9	28.0
MG	42.6	5.9	1.1	6.6	20.2
OSB	50.1	5.9	0.6	1.1	22.0
PLig	ND	ND	ND	ND	ND
PJ	51.8	6.0	0.5	3.2	23.1
ReCa	42.0	6.2	1.0	8.9	20.0
SW	ND	ND	ND	2.0	21.6
SG	45.4	5.9	0.5	3.9	ND
TP	47.4	6.0	0.2	0.4	ND
WO	45.5	5.0	0.2	4.7	24.0

[a]Lignin weight percent measured via mass spectral analysis.

Determining how variation in feedstock affects the downstream processes (catalyst deactivation, product composition, product distributions, etc.) is a formidable challenge that can be aided by chemometrics and statistical analysis (e.g., machine learning) once sufficiently large data sets are collected and organized. To evaluate the thermochemical conversion methods, rapid mass spectral analysis of feedstock pyrolysis vapors is well suited to predict changes in process outcomes dependent on feedstock composition.

In addition to demonstrating the value of high-throughput screening coupled with statistical analysis, these data provided specific insights into the effect of feedstocks on the vapor phase upgrading with the ZSM-5 catalyst. These data indicate that the total coke content on the ZSM-5 catalyst is not directly proportional to the degree of deactivation of the catalyst for the production of aromatics additionally, these data highlighted that pyrolysis vapors from grass clippings stood out as a particularly rapid deactivator of ZSM-5. Statistical analysis of the raw pyrolysis spectra leads to the hypothesis that this was due to the significant presence of nitrogen-containing compounds, likely from fertilizers, pesticides, and/or chlorophyll in this particular feedstock, not found in abundance in the other feedstocks. Rapid deactivation from the grass clippings may also be an indirect result of the high ash content of the sample due to ash-catalyzed reactions that increase the proportion of carbohydrate vapors that rapidly deactivate ZSM-5. This work highlights the value of rapid pyrolysis vapor screening of feedstocks using mass spectrometry to predict performance in a vapor-phase upgrading process.

■ ASSOCIATED CONTENT

Supporting Information

The Supporting Information is available free of charge at https://pubs.acs.org/doi/10.1021/acssuschemeng.1c05916.

Milligrams of coke on the catalyst *versus* the residual activity plotted for a subset of feedstocks; FP spectrum of grass clippings; and detailed description of the lignin isolation method (PDF)

■ AUTHOR INFORMATION

Corresponding Author

Anne K. Starace − *National Renewable Energy Laboratory, Golden, Colorado 80401, United States;* orcid.org/0000-0002-9204-2050; Email: Anne.Starace@nrel.gov

Authors

David D. Lee − *National Renewable Energy Laboratory, Golden, Colorado 80401, United States*

Kristen T. Hietala − *National Renewable Energy Laboratory, Golden, Colorado 80401, United States*

Yeonjoon Kim − *Chemistry Department, Colorado State University, Fort Collins, Colorado 80523, United States;* orcid.org/0000-0002-4784-7925

Seonah Kim − *Chemistry Department, Colorado State University, Fort Collins, Colorado 80523, United States;* orcid.org/0000-0001-9846-7140

Anne E. Harman-Ware − *National Renewable Energy Laboratory, Golden, Colorado 80401, United States;* orcid.org/0000-0002-7927-9424

Daniel L. Carpenter − *National Renewable Energy Laboratory, Golden, Colorado 80401, United States;* orcid.org/0000-0001-7625-9308

Complete contact information is available at: https://pubs.acs.org/10.1021/acssuschemeng.1c05916

Notes

The authors declare no competing financial interest.

■ ACKNOWLEDGMENTS

We would like to thank Rui Katahira for the preparation of pine lignin and Calvin Mukarakate for helpful discussions. Computer time for Y.K. and S.K. was provided by the Extreme Science and Engineering Discovery Environment (XSEDE), which is supported by the National Science Foundation grant number TG-CHE200128 and by the National Renewable Energy Laboratory Computational Sciences Center. We would also like to thank Idaho National Laboratory (INL) for providing the feedstocks for this study and their ash contents. This work was authored by the National Renewable Energy Laboratory, operated by Alliance for Sustainable Energy, LLC, for the U.S. Department of Energy (DOE) under contract no. DE-AC36-08GO28308. Funding provided by U.S. Department of Energy Office of Energy Efficiency and Renewable Energy Bioenergy Technologies Office. Funding was also provided by the Center for Bioenergy Innovation (CBI) from the U.S. Department of Energy Bioenergy Research Centers supported by the Office of Biological and Environmental Research in the DOE Office of Science. The views expressed in the article do not necessarily represent the views of the DOE or the U.S. Government. The U.S. Government retains and the publisher, by accepting the article for publication, acknowledges that the U.S. Government retains a nonexclusive, paid-up, irrevocable, worldwide license to publish or reproduce the published form of this work, or allow others to do so, for U.S. Government purposes.

REFERENCES

(1) Mihalcik, D. J.; Mullen, C. A.; Boateng, A. A. Screening Acidic Zeolites for Catalytic Fast Pyrolysis of Biomass and Its Components. *J. Anal. Appl. Pyrolysis* **2011**, *92*, 224−232.

(2) Mante, O. D.; Agblevor, F. A. Catalytic pyrolysis for the production of refinery-ready biocrude oils from six different biomass sources. *Green Chem.* **2014**, *16*, 3364−3377.

(3) Wang, K.; Mante, O. D.; Peters, J. E.; Dayton, D. C. Influence of the Feedstock on Catalytic Fast Pyrolysis with a Solid Acid Catalyst. *Energy Technol.* **2017**, *5*, 183−188.

(4) Dutta, A.; Sahir, A.; Tan, E.; Humbird, D.; Snowden-swan, L. J.; Meyer, P.; Ross, J.; Sexton, D.; Yap, R.; Lukas, J.; et al. *Process Design and Economics for the Conversion of Lignocellulosic Biomass to Hydrocarbon Fuels Fast Pyrolysis Vapors Process Design and Economics for the Conversion of Lignocellulosic Biomass to Hydrocarbon Fuels Thermochemical Research Pathways with in*. 2015.

(5) Sluiter, J.; Sluiter, A. *Summative Mass Closure Laboratory Analytical Procedure (LAP) Review and Integration*; National Renewable Energy Laboratory, 2011; Vol. *2011*.

(6) Harman-Ware, A. E.; Foster, C.; Happs, R. M.; Doeppke, C.; Meunier, K.; Gehan, J.; Yue, F.; Lu, F.; Davis, M. F. A thioacidolysis method tailored for higher-throughput quantitative analysis of lignin monomers. *Biotechnol. J.* **2016**, *11*, 1268−1273.

(7) Sykes, R.; Yung, M.; Novaes, E.; Kirst, M.; Peter, G.; Davis, M. High-Throughput Screening of Plant Cell-Wall Composition Using Pyrolysis Molecular Beam Mass Spectroscopy. In *Biofuels: Methods and Protocols*; Humana Press, 2009; pp 169−183.

(8) Decker, S. R.; Harman-Ware, A. E.; Happs, R. M.; Wolfrum, E. J.; Tuskan, G. A.; Kainer, D.; Oguntimein, G. B.; Rodriguez, M.; Weighill, D.; Jones, P.; et al. High Throughput Screening Technologies in Biomass Characterization. *Front. Energy Res.* **2018**, *6*, 1−18.

(9) Harman-Ware, A. E.; Macaya-Sanz, D.; Abeyratne, C. R.; Doeppke, C.; Haiby, K.; Tuskan, G. A.; Stanton, B.; Difazio, S. P.; Davis, M. F. Accurate determination of genotypic variance of cell wall characteristics of a Populus trichocarpa pedigree using high-throughput pyrolysis-molecular beam mass spectrometry. *Biotechnol. Biofuels* **2021**, *14*, 1−15.

(10) Agblevor, F. A.; Evans, R. J.; Johnson, K. D. Molecular-beam mass-spectrometric analysis of lignocellulosic materials. *J. Anal. Appl. Pyrolysis* **1994**, *30*, 125−144.

(11) Davis, M.; Johnson, D.; Agblevor, F.; Fennell, J.; Ashley, P. Variability in the Composition of Short Rotation Woody Feedstocks. In *Second Biomass Conference of the Americas: Energy, Environment, Agriculture, and Industry*, 1995; pp 216−225.

(12) Jarvis, M. W.; Haas, T. J.; Donohoe, B. S.; Daily, J. W.; Gaston, K. R.; Frederick, W. J.; Nimlos, M. R. Elucidation of Biomass Pyrolysis Products Using a Laminar Entrained Flow Reactor and Char Particle Imaging. *Energy Fuels* **2011**, *25*, 324−336.

(13) Mukarakate, C.; Zhang, X.; Stanton, A. R.; Robichaud, D. J.; Ciesielski, P. N.; Malhotra, K.; Donohoe, B. S.; Gjersing, E.; Evans, R. J.; Heroux, D. S.; et al. Real-Time Monitoring of the Deactivation of HZSM-5 during Upgrading of Pine Pyrolysis Vapors. *Green Chem.* **2014**, *16*, 1444.

(14) Nag, A.; Gerritsen, A.; Doeppke, C.; Harman-Ware, A. E. Machine Learning-Based Classification of Lignocellulosic Biomass from Pyrolysis-Molecular Beam Mass Spectrometry Data. *Int. J. Mol. Sci.* **2021**, *22*, 4107.

(15) Xiao, L.; Wei, H.; Himmel, M. E.; Jameel, H.; Kelley, S. S. NIR and Py-mbms coupled with multivariate data analysis as a high-throughput biomass characterization technique: a review. *Front. Plant Sci.* **2014**, *5*, 1−10.

(16) Sykes, R. W.; Gjersing, E. L.; Doeppke, C. L.; Davis, M. F. High-Throughput Method for Determining the Sugar Content in Biomass with Pyrolysis Molecular Beam Mass Spectrometry. *BioEnergy Res.* **2015**, *8*, 964−972.

(17) Bjorkman, A. Studies on Finely Divided Wood. Part I. Extractions of Lignin with Neutral Solvents. *Sven. Papperstidning* **1957**, *60*, 158.

(18) Chang, H.-m.; Cowling, E. B.; Brown, W.; Comparative Studies on Cellulolytic Enzyme Lignin and Milled Wood Lignin of Sweetgum and Spruce. *Holzforschunq* **1975**, *29*.153 doi:

(19) Evans, R. J.; Milne, T. a. Molecular characterization of the pyrolysis of biomass. *Energy Fuels* **1987**, *1*, 123−137.

(20) Cheah, S.; Malone, S. C.; Feik, C. J. Speciation of Sulfur in Biochar Produced from Pyrolysis and Gasification of Oak and Corn Stover. *Environ. Sci. Technol.* **2014**, *48*, 8474−8480.

(21) Howe, D.; Westover, T.; Carpenter, D.; Santosa, D.; Emerson, R.; Deutch, S.; Starace, A.; Kutnyakov, I.; Lukins, C. Field-to-Fuel Performance Testing of Lignocellulosic Feedstocks: An Integrated Study of the Fast Pyrolysis-Hydrotreating Pathway. *Energy Fuel.* **2015**, *29*, 3188−3197.

(22) Howe, D. T.; Westover, T.; Carpenter, D.; Santosa, D.; Emerson, R.; Deutch, S.; Starace, A.; Kutnyakov, I.; Lukins, C.; Kutnyakov, I. Field-to-Fuel Performance Testing of Lignocellulosic Feedstocks: An Integrated Study of the Fast Pyrolysis-Hydrotreating Pathway. *Biomass Bioenergy* **2015**, *29*, 3188.

(23) Martens, H.; Martens, M. Modified Jack-Knife Estimation of Parameter Uncertainty in Bilinear Modelling by Partial Least Squares Regression (PLSR). *Food Qual. Prefer.* **2000**, *11*, 5−16.

(24) Pedregosa, F.; Varoquaux, G.; Gramfort, A.; Michel, V.; Thirion, B.; Grisel, O.; Blondel, M.; Prettenhofer, P.; Weiss, R.; Dubourg, V.; Pedregosa, F.; Varoquaux, G.; Gramfort, A.; Michel, V.; Thirion, B.; Grisel, O.; Blondel, M.; Prettenhofer, P.; Weiss, R. Scikit-Learn : Machine Learning in Python. *J. Mach. Learn. Res.* **2011**, *12*, 2825−2830.

(25) Wang, K.; Kim, K. H.; Brown, R. C. Catalytic pyrolysis of individual components of lignocellulosic biomass. *Green Chem.* **2014**, *16*, 727−735.

(26) Stanton, A. R.; Iisa, K.; Mukarakate, C.; Nimlos, M. R. Role of Biopolymers in the Deactivation of ZSM-5 during Catalytic Fast Pyrolysis of Biomass. *ACS Sustain. Chem. Eng.* **2018**, *6*, 10030−10038.

(27) National Institute of Standards and Technology. *NIST Chemistry WebBook, NIST Standard Reference Database Number 69*; Mallard, P. J. L., Ed.; NIST: Gaithersburg MD, 2021.

(28) Caeiro, G.; Magnoux, P.; Ayrault, P.; Lopes, J.; Ribeiro, F. Deactivating Effect of Coke and Basic Nitrogen Compounds during the Methylcyclohexane Transformation over H-MFI Zeolite. *Chem. Eng. J.* **2006**, *120*, 43−54.

(29) Cerqueira, H. S.; Caeiro, G.; Costa, L.; Ramoa Ribeiro, F. Deactivation of FCC catalysts. *J. Mol. Catal. A: Chem.* **2008**, *292*, 1−13.

(30) Harman-Ware, A. E.; Morgan, T.; Wilson, M.; Crocker, M.; Zhang, J.; Liu, K.; Stork, J.; Debolt, S. Microalgae as a renewable fuel source: Fast pyrolysis of Scenedesmus sp. *Renewable Energy* **2013**, *60*, 625−632.

(31) Ralph, J.; Lundquist, K.; Brunow, G.; Lu, F.; Kim, H.; Schatz, P. F.; Marita, J. M.; Hatfield, R. D.; Ralph, S. A.; Christensen, J. H.; et al. Lignins: Natural polymers from oxidative coupling of 4-hydroxyphenyl- propanoids. *Phytochem. Rev.* **2004**, *3*, 29−60.

(32) Patwardhan, P. R.; Satrio, J. A.; Brown, R. C.; Shanks, B. H. Influence of Inorganic Salts on the Primary Pyrolysis Products of Cellulose. *Bioresour. Technol.* **2010**, *101*, 4646−4655.

(33) Wang, K.; Zhang, J.; Shanks, B. H.; Brown, R. C. The Deleterious Effect of Inorganic Salts on Hydrocarbon Yields from Catalytic Pyrolysis of Lignocellulosic Biomass and Its Mitigation. *Appl. Energy* **2015**, *148*, 115−120.

(34) Starace, A. K.; Evans, R. J.; Lee, D. D.; Carpenter, D. L. Effects of Torrefaction Temperature on Pyrolysis Vapor Products of Woody and Herbaceous Feedstocks. *Energy Fuel.* **2016**, *30*, 5677.

(35) Yoo, C. G.; Kim, H.; Lu, F.; Azarpira, A.; Pan, X.; Oh, K. K.; Kim, J. S.; Ralph, J.; Kim, T. H. Understanding the Physicochemical Characteristics and the Improved Enzymatic Saccharification of Corn Stover Pretreated with Aqueous and Gaseous Ammonia. *BioEnergy Res.* **2016**, *9*, 67−76.

(36) Ralph, J. Hydroxycinnamates in Lignification. *Phytochem. Rev.* **2010**, *9*, 65−83.

https://doi.org/10.1021/acssuschemeng.1c05916
ACS Sustainable Chem. Eng. XXXX, XXX, XXX−XXX

(37) Ralph, J.; Brunow, G.; Boerjan, W. *Encyclopedia of Life Sciences*; John Wiley & Sons, 2007.

https://doi.org/10.1021/acssuschemeng.1c05916
ACS Sustainable Chem. Eng. XXXX, XXX, XXX−XXX